tum stays fixed (Fig. 6). This motion does not affect the average space-group symmetry. Therefore there is no reason to expect coupling between translation and uniaxial rotation to exist and affect the observed Bragg reflexions. On the contrary, by looking at Fig. 6, one can see that $-C\equiv N$ reorientations cannot occur without a huge local distortion of the crystal lattice. Fig. 4 shows a molecule aligned in the [010] direction and the same one after such a reorientation around *G*. If we want to put this molecule in an equilibrium position again, we must translate it by $OO' = 0{\cdot}78$ Å. These two reasons clearly indicate that a strong coupling exists between translations and reorientations of the $C\equiv N$ group. The influence of this strong coupling on experimental results remains small only because its frequency is very small, of the order of 400 kHz at room temperature (Amoureux, Bee & Castelain, 1979*a*).

The authors thank M Odou for measuring the intensities, and Mme Carpentier and M Muller for growing the single crystals. We thank also MM Baert, Damien and Devos for their friendly advice.

References

AMOUREUX, J. P. & BEE, M. (1979*a*). To be published.
AMOUREUX, J. P. & BEE, M. (1979*b*). To be published.
AMOUREUX, J. P., BEE, M. & CASTELAIN, M. (1979*a*). To be published.
AMOUREUX, J. P., BEE, M. & CASTELAIN, M. (1979*b*). To be published.
AMOUREUX, J. P., BEE, M., CASTELAIN, M., ARNAUD, B. & SCHOUTEETEN, M. L. (1979). *J. Magn. Reson.* Submitted.
AMOUREUX, J. P., BEE, M. & DAMIEN, J. C. (1979). To be published.
CHADWICK, D., LEGON, A. C. & MILLEN, D. J. (1972). *J. Chem. Soc. Faraday Trans.* **68**, 2064–2069.
International Tables for X-ray Crystallography (1959). Vol. II. Birmingham: Kynoch Press.
PRESS, W. & HÜLLER, A. (1973). *Acta Cryst.* A**29**, 252–256.
SCHOMAKER, V. & TRUEBLOOD, K. N. (1968). *Acta Cryst.* B**24**, 63–76.
WILLIS, B. T. M. & PAWLEY, G. S. (1969). *Acta Cryst.* A**26**, 254–262.

Acta Cryst. (1979). B**35**, 2962–2966

Dimethylglyoxime: a Restricted X-ray Charge-Density Refinement

BY B. M. CRAVEN, C. H. CHANG AND D. GHOSH

Department of Crystallography, University of Pittsburgh, Pittsburgh, Pennsylvania 15260, *USA*

(*Received* 21 *May* 1979; *accepted* 30 *July* 1979)

Abstract

Crystals of dimethylglyoxime ($C_4H_8N_2O_2$) are triclinic, space group $P\bar{1}$ with $a = 6{\cdot}075\,(3)$, $b = 6{\cdot}314\,(3)$, $c = 4{\cdot}484\,(2)$ Å, $\alpha = 122{\cdot}50\,(3)$, $\beta = 91{\cdot}66\,(4)$, $\gamma = 77{\cdot}75\,(3)°$ with one molecule per cell. The structure has been redetermined from 521 X-ray intensities measured with Cu $K\alpha$ radiation ($\sin\theta/\lambda \leq 0{\cdot}60$ Å^{-1}). After a conventional least-squares refinement ($R = 0{\cdot}034$), population parameters were introduced for octapole deformations of spherical Hartree–Fock C, N and O atoms in order to fit apparent residual bonding charge density. The agreement improved significantly ($R = 0{\cdot}025$). Charge deformations in the oxime group were found to be trigonal for N and tetrahedral for O.

Introduction

McCrone (1949) reported morphological and optical properties for dimethylglyoxime (Fig. 1) and measured the X-ray cell data. Merritt & Lanterman (1952) determined the crystal structure (Fig. 2) from X-ray photographic intensity data. Hamilton (1961) used neutron *hk*0 and 0*kl* data to show that the molecules in the structure existed in the hydroxyimino tautomeric form.

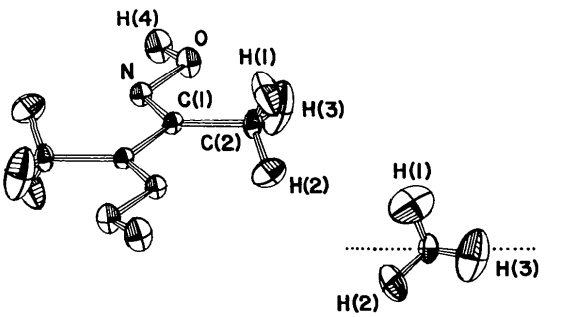

Fig. 1. Molecular structure and atomic nomenclature for dimethylglyoxime. Thermal parameters are represented as 25% probability ellipsoids. In the view of the methyl group down the C(1)–C(2) bond, the trace of the molecular plane is shown as a dotted line.

0567-7408/79/122962-05$01.00

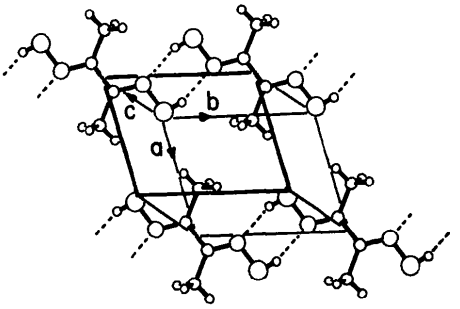

Fig. 2. The crystal structure of dimethylglyoxime in projection on the (101) plane. The four molecules belong to the same almost planar sheet.

The methyl H atoms were not accurately located because of suspected systematic errors.

We report a redetermination of the X-ray structure from diffractometer data collected with Cu $K\alpha$ radiation ($\sin\theta/\lambda \leq 0{\cdot}6$ Å^{-1}). This was carried out as part of a student instructional program* which included demonstrating the usual structure refinement with scattering factors for isolated spherical neutral atoms. Further refinement came from observing significant features in the residual electron density map which might represent chemical bonding. Most of the valence-shell Bragg scattering occurs within the angular range accessible with Cu $K\alpha$ radiation. However, it is difficult to isolate these effects without having additional X-ray or neutron intensity data for determining the nuclear positions and thermal motion. In structure refinements using the rigid pseudoatom model (Stewart, 1976), the electronic charge density about each nuclear center is represented as a sum of multipole terms each with an electron population parameter which can be determined by least-squares methods. Others have used similar procedures (Hirshfeld, 1977; Hansen & Coppens, 1978). When only Cu $K\alpha$ data are available, strong correlations are expected between the usual atomic positional and thermal parameters and certain of the charge parameters. Particularly for H atoms, a shift in apparent position may mask a dipole deformation of charge density. Anisotropic thermal parameters may absorb a quadrupole charge deformation. For dimethylglyoxime, most of the residual electron density has been incorporated in the structure model by introducing seven parameters per atom to describe octapole charge deformations at the C, N and O atoms. Although structure models such as the L-shell projection (Stewart, 1970) have been used to determine net atomic charges in cases where only low-angle X-ray diffraction data are available (Ruble, Wang & Craven, 1979) we are unaware of similar refinements in which aspherical atomic-charge distributions are assumed.

* Dimethylglyoxime is well suited for this purpose. The crystals are stable and easily obtained with well developed faces. The structure is simple (asymmetric unit C_2H_4NO) but the triclinic symmetry and twinning provide a challenging exercise in precession photography. The planar molecular framework is revealed with a single superposition using the Patterson section which we provide as a supplementary figure (see deposition footnote).

Experimental

(*a*) *Data collection*

Triclinic crystals of dimethylglyoxime grown by evaporation of an ethanolic solution were commonly twinned on (101) which is parallel to the almost planar layers of molecules in the structure (Fig. 2).† For X-ray data collection a single crystal was cut from a twin to form a triangular (100) plate, 0·4 mm on its long edges and 0·08 mm thick. The crystal was mounted with c^* along the φ axis of a computer-controlled four-circle diffractometer. Graphite-monochromated Cu $K\alpha$ radiation ($\lambda = 1{\cdot}5418$ Å) was used. Lattice parameters had room-temperature values $a = 6{\cdot}075\,(3)$, $b = 6{\cdot}314\,(3)$, $c = 4{\cdot}484\,(2)$ Å, $\alpha = 122{\cdot}50\,(3)$, $\beta = 91{\cdot}66\,(4)$, $\gamma = 77{\cdot}75\,(3)°$, obtained by least-squares fitting to $\sin^2\theta$ values for 23 reflections measured at $\pm\theta$. This cell was chosen to be consistent with the previous literature. The Niggli reduced cell ($a = 4{\cdot}482$, $b = 5{\cdot}435$, $c = 6{\cdot}075$ Å, $\alpha = 102{\cdot}86$, $\beta = 91{\cdot}66$, $\gamma = 101{\cdot}56°$) is obtained by the transformation (0, 0, 1/0, −1, −1/1, 0, 0). Integrated intensities were measured at room temperature for 521 non-symmetry-related reflections with $\sin\theta/\lambda \leq 0{\cdot}60$ Å^{-1} using $\theta/2\theta$ scans. The variance in an intensity was assumed to be $\sigma(I) = \sigma^2 + (0{\cdot}02I)^2$ where σ^2 is the variance from counting statistics. Integrated intensities for the two strong reflections 001 and 101 were also measured at 30° intervals of crystal rotation about the Bragg vector. There was an almost sinusoidal variation of 15 and 45% from the respective maximum intensity values.‡ Since these variations were greater than could be attributed to X-ray absorption ($\mu = 0{\cdot}885$ mm^{-1}), we believed that a secondary-extinction parameter would be justified in the structure refinement. All intensity data were corrected for absorption§ by a numerical integration procedure (Busing & Levy, 1957) which also gave the absorption-weighted path lengths ($\bar{t}$) required for the extinction corrections.

(*b*) *The conventional structure refinement*

All refinements to be described were carried out by a full-matrix least-squares method using the computer

† The twin plane was reported as (001) by McCrone (1949).

‡ Intensities were measured similarly for the weak reflection 002. All values were within $1{\cdot}5\sigma$ of the average intensity.

§ Crystal faces and their distances (mm) from a common origin were (100), 0·04; ($\bar{1}$00), 0·04; (0$\bar{1}$0), 0·10; (01$\bar{1}$), 0·10; (001), 0·09.

programs of Craven & Weber (1978). The function minimized was $\sum w\Delta^2$ where $\Delta = |F_o| - |F_c|$ and $w = \sigma^{-2}(F_o)$. X-ray scattering factors derived from Hartree–Fock wavefunctions for neutral isolated spherical atoms were those of Cromer & Waber (1965) for C, N and O and Stewart, Davidson & Simpson (1965) for spherically averaged bonded H.

The conventional refinement began with variables consisting of a scale factor and the heavier-atom positional and anisotropic thermal parameters with the initial values of Merritt & Lanterman (1952). Fixed neutron values were assumed for the H atoms (Hamilton, 1961). Extinction effects became apparent at an early stage. When an isotropic extinction parameter was introduced, assuming a type I crystal with a Lorentzian distribution of mosaicity (Becker & Coppens, 1974), the refinement converged at $R = 0{\cdot}055$, $R_w = 0{\cdot}087$.* In an $(F_o - F_c)$ Fourier map there were peaks of 0·15 e Å^{-3} between the methyl H atoms. In a second map, with H atoms omitted from F_c, the methyl H atoms appeared as three well resolved peaks. However, the group was turned from the neutron positions 15° anticlockwise about the C(2)–C(1) bond, so as to bring H(3) almost into the molecular plane (Fig. 1). From this map the H-atom thermal vibrations seemed to be large, but there was no basis for considering a disordered model. Refinement including H-atom positional and anisotropic thermal parameters as variables gave convergence at $R = 0{\cdot}034$, $R_w = 0{\cdot}048$. According to the R-factor ratio test (Hamilton, 1974) the H-atom refinement could be taken as an improvement in the structure model with greater than 99·5% confidence. The new results are not surprising, since Hamilton (1961) suspected the methyl H-atom positions to be inaccurately determined due to unidentified systematic errors in the neutron data.

(c) *The charge-deformation refinement*

The $(F_o - F_c)$ Fourier map after the conventional refinement showed residual features (~0·15 e Å^{-3}) which were highly significant in terms of the e.s.d. in the observed electron density (0·02 e Å^{-3}). Peaks previously noted between the methyl H atoms were gone, but others remained which were consistent with directed bonding density either trigonally or tetrahedrally disposed about the C, N and O atoms. The refinement was concluded with these features represented by octapolar charge deformations (Stewart, 1976) superposed on the spherical Hartree–Fock atoms. The X-ray scattering factors became $f = f_{HF} - if_o[o_1(s_x^2 - 3s_y^2)s_x + o_2(3s_x^2 - s_y^2)s_y + o_3(s_x^2 - s_y^2)s_z + o_4 \times s_x s_y s_z + o_5(5s_z^2 - 1)s_x + o_6(5s_z^2 - 1)s_y + o_7(5s_z^2 - 3)s_z]$ where f_{HF} is the scattering from Hartree–Fock atoms, $i = (-1)^{1/2}$, s_x, s_y, s_z are the direction cosines of the Bragg vector with respect to the crystal axial system **a**, **c*** × **a**, **c*** and the seven population parameters o_j for each C, N and O atom are least-squares variables. The octapole radial scattering factor $f_o = (16c^3/5)(1 + c^2)^{-5}$, where $c = (4\pi/\alpha)(\sin\theta/\lambda)$, comes from an assumed Slater-type radial charge distribution (Epstein & Stewart, 1977). The radial parameter α was assigned standard values (Hehre, Stewart & Pople, 1969) of 6·43, 7·37 and 8·50 Å^{-1} for C, N and O respectively. Hydrogen scattering factors were unchanged.

The refinement converged† with $R = 0{\cdot}025$, $R_w = 0{\cdot}034$ and quadratic mean error $[(\sum w\Delta^2)/(m-n)]^{1/2} = 2{\cdot}32$. The final $(F_o - F_c)$ map contained a peak 0·13 e Å^{-3} at the midpoint of the H(4)···N hydrogen bond, but no other features were more than possibly significant (4σ).† There were negligible changes in the atomic positional parameters (Table 1), the largest being $2{\cdot}2\sigma$ in the value of x for the O atom. Values of most thermal parameters U_{ij} decreased slightly ($\leq 4\sigma$).

* $R = \sum|\Delta|/\sum|F_o|$; $R_w = (\sum w\Delta^2/\sum wF_o^2)^{1/2}$.

† A list of structure factors and figures showing the final $(F_o - F_c)$ map, and the Patterson function have been deposited with the British Library Lending Division as Supplementary Publication No. SUP 34711 (10 pp.). Copies may be obtained through The Executive Secretary, International Union of Crystallography, 5 Abbey Square, Chester CH1 2HU, England.

Table 1. *Atomic parameters*

(*a*) Positional parameters

Fractional coordinates are × 10^4 for C, N and O and × 10^3 for H atoms.

	x	y	z
C(1)	897 (1)	171 (2)	−875 (2)
C(2)	2954 (2)	−1966 (2)	−2913 (3)
N	519 (1)	2388 (2)	−484 (2)
O	2240 (1)	2657 (2)	−2191 (2)
H(1)	388 (4)	−235 (5)	−143 (7)
H(2)	256 (4)	−363 (4)	−445 (7)
H(3)	395 (4)	−164 (4)	−412 (6)
H(4)	171 (4)	426 (4)	−154 (6)

(*b*) Anisotropic thermal parameters

These are defined according to the temperature-factor expression $T = \exp(-2\pi^2 \sum_i \sum_j h_i h_j a_i^* a_j^* U_{ij})$ with U_{ij} values in Å^2 × 10^4 for C, N and O and Å^2 × 10^3 for H atoms.

	U_{11}	U_{22}	U_{33}	U_{12}	U_{13}	U_{23}
C(1)	341 (5)	258 (5)	375 (5)	−46 (3)	−12 (3)	202 (4)
C(2)	390 (6)	321 (6)	580 (6)	20 (4)	96 (5)	274 (5)
N	375 (5)	296 (5)	451 (5)	−58 (3)	16 (3)	252 (4)
O	448 (5)	380 (5)	674 (5)	−44 (3)	114 (3)	368 (4)
H(1)	51 (11)	143 (21)	116 (18)	21 (12)	6 (11)	81 (17)
H(2)	93 (14)	46 (11)	107 (16)	−18 (11)	−7 (12)	23 (12)
H(3)	100 (17)	78 (14)	109 (17)	12 (12)	58 (13)	58 (13)
H(4)	89 (13)	55 (13)	126 (16)	−6 (11)	16 (11)	58 (13)

(*c*) Electron population parameters (× 10)

Scattering factors corresponding to octapole deformations of charge density are defined according to the equation given in the text.

	o_1	o_2	o_3	o_4	o_5	o_6	o_7
C(1)	−6 (1)	−6 (1)	11 (2)	20 (6)	−4 (1)	2 (1)	0 (1)
C(2)	4 (1)	3 (2)	−1 (4)	−32 (9)	3 (1)	−1 (1)	2 (1)
N	3 (1)	4 (1)	−14 (2)	−14 (5)	2 (1)	1 (1)	1 (1)
O	0 (1)	−5 (1)	−2 (3)	9 (5)	1 (1)	3 (1)	2 (1)

There was at least one significantly non-zero population parameter (o_j) for each non-H atom. The least-squares parameter correlations involving o_j were all less than 0·5. By the R-factor ratio test (Hamilton, 1974), the improved agreement achieved by including these 28 parameters can be accepted with greater than 99·5% confidence.

Extinction was found to be moderately severe, giving $g = 264\ (23)\ \text{rad}^{-1}$. The reflection 101 was most affected ($0{\cdot}61F_c$) among the eleven with correction factors less than 0·95. When extinction corrections were included in F_c, there was good agreement with $|F_o|$ as a function of crystal rotation about the Bragg vectors 101 and 001.

Discussion

Except for the revised H-atom configuration, the atomic distances and angles (Table 2) are in agreement with those of Merritt & Lanterman (1952) and Hamilton (1961). Since the thermal parameters for the C, N and O atoms are in agreement with rigid-body behavior (Schomaker & Trueblood, 1968), bond lengths for these atoms (Table 2) are corrected for rigid-body libration (Table 3).

Atoms of the molecular framework are very close to the best least-squares plane, $3{\cdot}2941x - 0{\cdot}0222y + 3{\cdot}3526z = 0$, which is nearly parallel to (101). The plane equation is referred to the crystal axes with x,y,z as fractional coordinates. Atomic displacements from the plane are 0·002, 0·001, 0·003 and −0·003 Å (e.s.d. = 0·001 Å) for atoms C(1), C(2), N and O and 0·04 (2) Å for H(4). Molecules are linked to form ribbons along the b direction by means of hydrogen bonds O–H(4)···N (Table 2). The ribbons are assembled in nearly planar sheets parallel to (101) at a spacing of 3·33 Å (Fig. 2).

The octapole charge deformation density is shown (Fig. 3) for the section in the best least-squares plane as defined above, and for a parallel section displaced by 0·4 Å. These maps were obtained by a computer program (Craven & Weber, 1978) which sums at each point the deformation terms from all atoms in the crystal centered within 2·5 Å of the point. The atoms are assumed to be at rest. Thus the atomic thermal motions must be properly determined in order that the deconvoluted deformation density in Fig. 3 can accurately represent features of the static charge distribution. The U_{ij} values are probably subject to systematic errors from taking up at least part of the quadrupole charge deformations, which have otherwise been neglected. However, such errors only have a significant effect on the charge density within about 0·3 Å of each atom center (Stewart, 1968). There may be systematic errors in the octapole population parameters due to the neglect of third-order atomic thermal parameters. Although difficult to assess, such errors are not believed to be important (Craven & McMullan, 1979). Except for being incomplete, Fig. 3 is considered to be a reasonably accurate map of the static charge distribution. It must be remembered that there is no contribution from the H atoms. This

Table 2. *Distances and angles*

(*a*) Bond distances*

	d_1	d_2		d_1
C(1)–C(1)′	1·477 (1) Å	1·483 Å	C(1)–H(1)	0·96 (3) Å
C(1)–C(2)	1·498 (2)	1·505	C(1)–H(2)	0·98 (3)
C(1)–N	1·283 (1)	1·287	C(1)–H(3)	0·95 (3)
N–O	1·403 (1)	1·409	O–H(4)	0·87 (3)

(*b*) Bond angles*

C(1)′–C(1)–C(2)	120·6 (1)°	C(1)–C(2)–H(1)	113 (2)°
C(1)′–C(1)–N	114·5 (1)	C(1)–C(2)–H(2)	112 (2)
C(2)–C(1)–N	124·8 (1)	C(1)–C(2)–H(3)	115 (2)
C(1)–N–O	113·4 (1)	H(1)–C(2)–H(2)	99 (2)
N–O–H(4)	99 (2)	H(1)–C(2)–H(3)	104 (2)
		H(2)–C(2)–H(3)	113 (2)

(*c*) Bond torsion angles

C(1)′–C(1)–N–O	−179·6 (1)°
C(2)–C(1)–N–O	0·3 (1)
C(1)–N–O–H(4)	−177 (2)
C(1)′–C(1)–C(2)–H(1)	−66 (2)
C(1)′–C(1)–C(2)–H(2)	45 (2)
C(1)′–C(1)–C(2)–H(3)	175 (2)

(*d*) Hydrogen bond O–H(4)···N

O···N	2·810 (1) Å	H···N	1·98 (3) Å
O–H···N	158 (2)°		

(*e*) Shortest intermolecular distances

C(1)···C(1)	$(-x, -y, -1-z)$	3·73 Å
C(1)···N	$(-x, -y, -1-z)$	3·41
C(2)···C(2)	$(1-x, -1-y, -1-z)$	3·59
H(1)···H(2)	$(1-x, -1-y, -1-z)$	2·72

* Distances d_1 are between thermal centroids. Distances d_2 are after correction for rigid-body libration. The corresponding angle corrections were <0·1°.

Table 3. *Thermal parameters for rigid-body motion*

Values are with respect to the crystal axial system **a**, **c*** × **a**, **c***. The r.m.s. difference 0·010 Å² was obtained between observed U_{ij} and the calculated values assuming rigid-body motion.

(*a*) Translational tensor (Å²)

$$\mathbf{T} = \begin{pmatrix} 0{\cdot}0329\ (10) & 0{\cdot}0000\ (8) & 0{\cdot}0019\ (10) \\ & 0{\cdot}0212\ (9) & 0{\cdot}0000\ (8) \\ & & 0{\cdot}0349\ (13) \end{pmatrix}$$

r.m.s. principal values: 0·190, 0·178, 0·146 Å.

(*b*) Librational tensor (deg²)

$$\mathbf{L} = \begin{pmatrix} 13\ (3) & 4\ (2) & -4\ (2) \\ & 26\ (2) & 0\ (2) \\ & & 6\ (2) \end{pmatrix}$$

r.m.s. principal values: 5·2, 3·8, 2·1°.

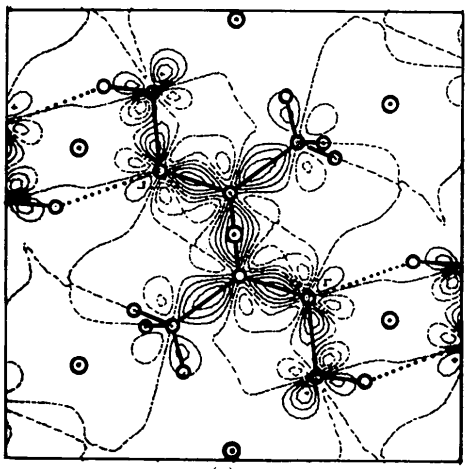

(*a*)

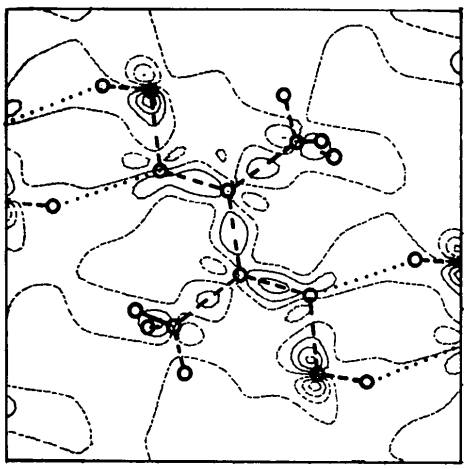

(*b*)

Fig. 3. Sections of the octapole deformation density. (*a*) Best least-squares plane through the C, N and O atoms. (*b*) Plane at 0·04 Å from (*a*). Contours are at intervals of 0·1 e Å^{-3} with solid lines for positive (excess) charge. The first broken contour is at zero. The maximum e.s.d. (0·08 e Å^{-3}) is near the O atom (see text). Crystallographic centers of symmetry are shown in (*a*).

deficiency in the structure model due to lack of extensive data, is probably the reason for the residual peak of 0·13 (2) e Å^{-3} which occurs along the H···N hydrogen bond in the final $(F_o - F_c)$ map.

The octapole deformation density in Fig. 3 nearly conforms to a molecular point symmetry of $2/m$, although only $\bar{1}$ is required by the space group. The lobes of positive deformation which overlap between bonded atoms are arranged trigonally about C(1) and N and tetrahedrally about C(2) and O. The deformation density at each bond center is 0·38 (3) e Å^{-3} at C(1)′–C(1), 0·38 (4) e Å^{-3} at C(1)–C(2) and 0·36 (5) e Å^{-3} at C(1)–N. The interesting difference is between the O and N atoms, each of which form only two covalent bonds. For the N atom, the positive deformation density is more strongly directed towards the bonded C(1) and O atoms, where peak values are 0·37 (5) e Å^{-3}, than into the H-bonding region, 0·20 (5) e Å^{-3}. The latter density might be enhanced if dipole charge deformations could be included. For the O atom, two of the tetrahedral positive-density lobes are in the molecular plane, one pointing towards the hydroxyl H(4) atom, 0·25 (7) e Å^{-3}, and the other into the non-bonding region, 0·41 (7) e Å^{-3}. The other positive lobes, 0·38 (6) e Å^{-3}, are directed towards the N atom, one on each side of the molecular plane.

It is not possible to carry out detailed studies of charge-density distributions in crystals using only room-temperature Cu $K\alpha$ X-ray data. However, such data are frequently collected for organic structures of moderate complexity, when the primary aim is to determine the atomic configuration. Dimethylglyoxime provides a simple example in which additional information concerning bonding charge density can be obtained from limited data at the expense of increased computing time. A favorable numerical ratio between least-squares variables (110) and observations (521) is retained.

This work was supported in part by a grant GM-22548 from the National Institutes of Health.

References

BECKER, P. J. & COPPENS, P. (1974). *Acta Cryst.* A**30**, 129–147.

BUSING, W. R. & LEVY, H. A. (1957). *Acta Cryst.* **10**, 180–182.

CRAVEN, B. M. & MCMULLAN, R. K. (1979). *Acta Cryst.* B**35**, 934–945.

CRAVEN, B. M. & WEBER, H. P. (1978). *The POP Least-Squares Refinement Procedure*, Technical Report, Crystallography Department, Univ. of Pittsburgh.

CROMER, D. T. & WABER, J. T. (1965). *Acta Cryst.* **18**, 104–109.

EPSTEIN, J. & STEWART, R. F. (1977). *J. Chem. Phys.* **66**, 4057–4064.

HAMILTON, W. C. (1961). *Acta Cryst.* **14**, 95–100.

HAMILTON, W. C. (1974). *International Tables for X-ray Crystallography*, Vol. IV, pp. 285–310. Birmingham: Kynoch Press.

HANSEN, N. K. & COPPENS, P. (1978). *Acta Cryst.* A**34**, 909–921.

HEHRE, W. J., STEWART, R. F. & POPLE, J. A. (1969). *J. Chem. Phys.* **51**, 2657–2664.

HIRSHFELD, F. L. (1977). *Isr. J. Chem.* **16**, 168–177.

MCCRONE, W. C. (1949). *Anal. Chem.* **21**, 1428–1429.

MERRITT, L. L. & LANTERMAN, E. (1952). *Acta Cryst.* **5**, 811–817.

RUBLE, J. R., WANG, A. C. & CRAVEN, B. M. (1979). *J. Mol. Struct.* **51**, 229–237.

SCHOMAKER, V. & TRUEBLOOD, K. N. (1968). *Acta Cryst.* B**24**, 63–76.

STEWART, R. F. (1968). *Acta Cryst.* A**24**, 497–505.

STEWART, R. F. (1970). *J. Chem. Phys.* **53**, 205–213.

STEWART, R. F. (1976). *Acta Cryst.* A**32**, 565–574.

STEWART, R. F., DAVIDSON, E. R. & SIMPSON, W. T. (1965). *J. Chem. Phys.* **42**, 3175–3187.